Electronic Supplementary Material (ESI) for ChemComm.

Supporting Information for

Conjugated microporous polymer based visual sensing platform for aminoglycoside antibiotic in water †

Subhajit Bhunia,‡ [a] Nilanjan Dey,‡ [b] Anirban Pradhan[a] Santanu Bhattacharya*[ab]
[a]Director's Research Unit, Indian Association for the Cultivation of Science, Kolkata 700032, India, **Email:** director@iacs.res.in
[b]Department of Organic Chemistry, Indian Institute of Science, Bangalore 560012 (India), Fax: (+91) 080-2360-0529, **E-mail:** sb@orgchem.iisc.ernet.in

‡Both authors contributed equally

Contents

Section S1

1. Experimental Section

1.1. Materials and methods

Perylene, bis(1,5-cyclooctadiene) di-iridium(I) dichloride and 4,4′-di-tert-butyl-2,2′-dipyridyl (dtbpy) were purchased from Aldrich, while bis(pinacolato)diboron (b_2pin_2), para-bromo-benzaldehyde, pyrrole were purchased from Spectrochem, India. Pyrrole was vacuum distilled prior to use. Nickel chloride, dioxane, acetone, cyclohexane, propionic acid, nitrobenzene etc. were received from Merck chemicals.

1.2. Characterization techniques

^{1}H and ^{13}C NMR was recorded using Bruker DPX-300 NMR spectrometer. The chemical shift (δ in ppm) was estimated with respect of the residual proton of the solvent as standard. Multiplicities are written as s (singlet), d (doublet), t (triplet), m (multiplet) and br (broad). The solid state cross-polarization magic angle spinning (CP-MAS) ^{13}C NMR spectrum was recorded using a 400MHz Bruker Avance II spectrometer at mass frequency of 8 kHz. FT-IR spectra were recorded using a Nicolet MAGNA-FT IR 750 Spectrometer Series II. Porosity measurement using volumetric N_2 adsorption/desorption at was carried out by Autosorb 1 (quantachrome, USA). Prior to adsorption analysis, the sample was outgassed at 130°C for 12 h to remove all the entrapped solvent impurities. NLDFT pore size distribution was obtained by applying slit/cylindrical pore model on the N_2 adsorption/desorption isotherm. Thermo gravimetric (TGA) and differential thermal analyses (DTA) of the samples were done by TGA Instruments thermal analyzer TA-SDT Q-600. TEM images were taken on a JEOL-JEM 2010 electron microscopy using 200kV electron source. TEM images on STEM (HAADF) were taken on a UHR-FEG-TEM, JEOL; JEM 2100 F model using 200kV electron source. The electron mapping data were collected using (Oxford EDS) in STEM (HAADF)-EDS probe line scan where the probe was of 0.2 nm. Specimens were prepared by dropping a drop of CMP dispersed solution in ethanol on a carbon coated copper grid, and the grid was dried under air. Photoelectron spectroscopy (XPS) experiment has been done by an Omicron nanotech operated at 15 kV and 20 mA. X-Ray diffraction patterns of the powder samples were obtained with a Bruker AXS D_8 Advanced SWAX diffractometer using Cu-Kα (0.15406 nm) radiation. . For the leeching test, the

supernatant phase was analyzed by using a Shimadzu AA-6300 atomic absorption spectrophotometer (AAS) fitted with a double beam monochromator.

1.3. Synthesis and procedures

1.3.1. Synthesis of nickel (II) 5,10,15,20-tetrakis-(4'-bromophenyl) porphyrin (Ni-POR)

This compound has been synthesized via a previously reported procedure.[1]

1.3.2. Synthesis of 2,5,8,11-tetrakis(4,4,5,5-tetramethyl-1,3,2-dioxaborolan-2-yl) perylene (P-bpin$_4$)

P-bpin$_4$ was synthesized via slight modification of the previously reported procedure.[2] Perylene (504.18 mg, 2 mmol), (1,5-Cyclooctadiene)(methoxy)iridium (I) dimer (61.17 mg, 0.1 mmol), dtbpy (80.2 mg, 0.3 mmol), and b_2pin_2 (3.05 g, 12 mmol) were dissolved in anhydrous cyclohexane (20 mL). Then the mixture was freeze dried under vacuum five times and the tube was backfilled with N_2 and reaction mixture was stirred at 80°C for 72 h under N_2 atmosphere. After completion of the reaction, the mixture was passed through a silica plug (eluent: $CHCl_3$) and the solvent was removed under reduced pressure. Purification of the residue by column chromatography (silica gel, hexane/$CHCl_3$ 1:1) afforded compound (1.3 g, 85 %) as a bright yellow solid. ^{1}H NMR (400 MHz, $CDCl_3$): 8.64 (s, 2H), 8.17 (d, J = 8.0 Hz, 2H), 8.11 (d, J = 9.0 Hz, 2H), 8.06 (d, J = 9.0 Hz, 2H), 8.02 (t, J = 8.0 Hz, 1H), 1.47 (s, 12H)

1.3.3. Synthesis of microporous PER@NiP-CMOP-1

198 mg (0.2 mmol) Ni-POR, 151 mg (0.2 mmol) P-bpin$_4$ and 60 mg $Pd(PPh)_3$ was dissolved in 20 ml dioxane/water mixture (4:1). Then 230 mg K_2CO_3 was added to the reaction flask and the mixture was degassed carefully via freeze-pump-thaw cycles three times to exclude all the dissolved oxygen present in the reaction mixture. The reaction mixture was heated to 80°C and stirred for 96 h under argon atmosphere. Then the mixture was cooled down to room temperature and poured into ice water. The purple precipitate was filtered and washed extensively by THF, methanol, acetone to remove the unwanted impurities (Improper washing can cause lower surface area). Then the precipitate was kept overnight under vacuum at 70°C to obtain the PER@NiP-CMOP-1 as fine purple powder (180 mg, ~98 %).

1.3.4. Procedure of optical sensing

For sensing studies, the well dispersed aqueous suspension of PER@NiP-CMOP-1 was taken (20 μg/mL) in water and the emission spectra in the presence of analytes were recorded without any time-lag. Similar procedures were also followed for the sensing in buffered media at different pH (HCO_2Na/HCl buffer for pH 2-4.5, NaOAc/HCl buffer for pH 4.5-6.5, Tris/HCl for pH 7-9 and $Na_2B_4O_7 \cdot 10H_2O$/NaOH for pH 9-10). The UV−vis and fluorescence spectroscopy were recorded on a Shimadzu model 2100 spectrometer and Cary Eclipse Spectro fluorimeter respectively. The slit-width for the fluorescence experiment was kept at 5 nm (excitation) and 5 nm (emission) and the excitation wavelength was set at 350 nm for PER@NiP-CMOP-1.

1.3.5. Fluorescence Decay Experiment

Fluorescence decay constants were measured by using a time-correlated single photon counting fluorimeter (Horiba Jobin Yvon). The system was excited with 400 nm nano LED of Horiba – Jobin Yvon with pulse duration of 1.2 ns (slit width of 2/2). The emission wavelength was fixed at both 470 and 600 nm. Average fluorescence decay time (τav) for the exponential iterative fitting were calculated from the decay times (τi) and the relative amplitudes (ai) using the following relation,

$\tau_{av} = (a_1\tau_{12} + a_2\tau_{22} + a_3\tau_{32})/ (a_1\tau_1 + a_2\tau_2 + a_3\tau_3)$

Where a_1, a_2 and a_3 are the relative amplitudes and τ_1, τ_2, and τ_3 are the lifetime values, respectively. For data fitting, a DAS_6 analysis software version 6.2 was used.

1.3.6. Reusability test of PER@NiP-CMOP-1 sensor

After each sensing experiment, the PER@NiP-CMOP-1 dispersed aqueous phase was diluted with acetone (2 times of aqueous phase) and then the mixture was centrifuged with 12000 rpm for 5 min. Then the supernatant upper layer was discarded and the settled solid was dried under vacuum (open air can cause the oxide formation of nickel) for overnight which was used for next experiment.

1.3.7. Leeching test of PER@NiP-CMOP-1 sensor

To confirm the robustness of the porous sensor, the upper supernatant layer after centrifugation of aqueous acetone mixture of PER@NiP-CMOP-1 was subjected to the atomic absorption spectroscopy technique which confirms about no nickel leeching was occurring from the CMP framework during recyclability.

References

1. L. Chen, Y. Yang and D. Jiang, *J. Am. Chem. Soc.,* 2010, **132**, 9138-9143.

2. D. N. Coventry, A. S. Batsanov, A. E. Goeta, J. A. K. H. Howard, T. B. Marder and R. N. Perutz, *Chem. Commun.*, 2005,**0**, 2172.

Section S2

System	Mode of sensing	Reversibility	Time required	Linear range	Detection limit	reference
Modified-RNA Aptamer-Based Impedimetric Assay	Change in impendence	Irreversible system (expensive method required RNA aptamer)	5 min	0.75-500 µM	Sub-micromolar	*J. Am. Chem. Soc* 2007, **129**, 3808-3809
RNA aptamer-based fluorimetric assay	Change in fluorescence	Irreversible system (expensive method required RNA aptamer)	10 min	0.1 to 10 µM	0.01 µM	*Anal Bioanal Chem.* 2016, **408**, 3593-600
Au NPs/carbon nanotube based immunosensor	Change in current	Irreversible system (expensive method required amperometer)	30 min	10 ng/mL and 250 ng/mL	6.76 ± 0.17 ng/mL	*Biosens. Bioelectron.* 2010, **26**,1002–1008
Melamine modified gold nanoparticles	Change in color	Not mentioned (Homogeneous system)	5 min	5 to 100 nM	30 pM	*Microchim Acta*, 2015, **182**, 1501–1507
Polydiacetylene based supramolecules	Change in color	Not mentioned (Homogeneous system)	5 min	0-10 µM	0.25 µM	*Macromol. Rapid Commun.* 2013, **34**, 944–948
polydiacetylene–phospholipids supramolecules	Change in color	Not mentioned (Homogeneous system)	20 min at 37 °C	0.1 to 50 µM	61 ppb	*Chem. Commun.*, 2012, **48**, 5313–5315
Nickel-based conjugated mesoporous polymer	Turn-on emission change	Recyclable heterogeneous sensing system	rapid	0-3 mM	0.22 µM	Present work*

Table S1. Table shows a comparison of the present method with other literature-reported procedures. The present method describes a unique example of rapid, recyclable, heterogeneous sensing system for neomycin.

Section S3

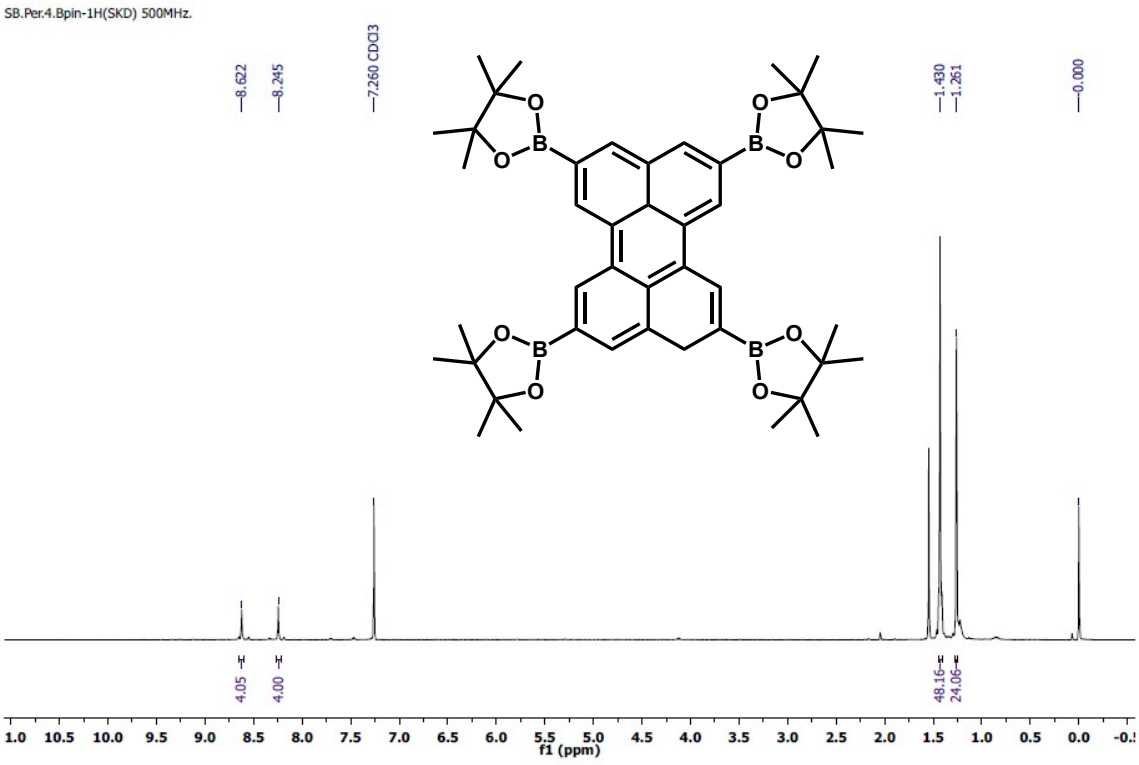

Figure S1. ^{1}H-NMR spectrum of 2,5,8,11- tetrakis (4,4,5,5-tetramethyl-1,3,2-dioxaborolan-2-yl) perylene (**P-bpin$_4$**) in $CDCl_3$.

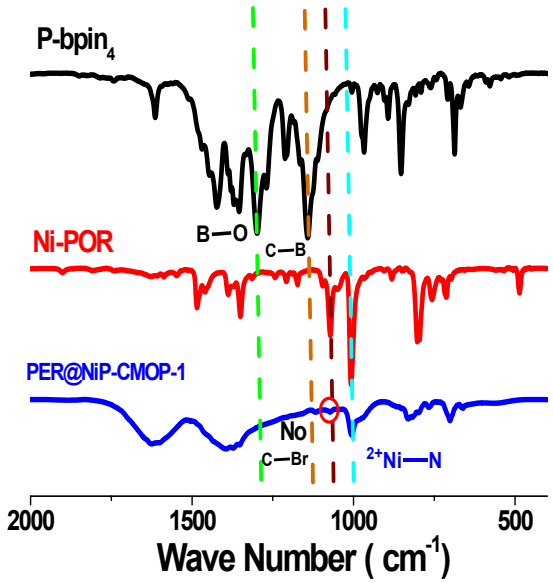

Figure S2. FTIR spectra of P-bpin$_4$, Ni-POR and **PER@NiP-CMOP-1**

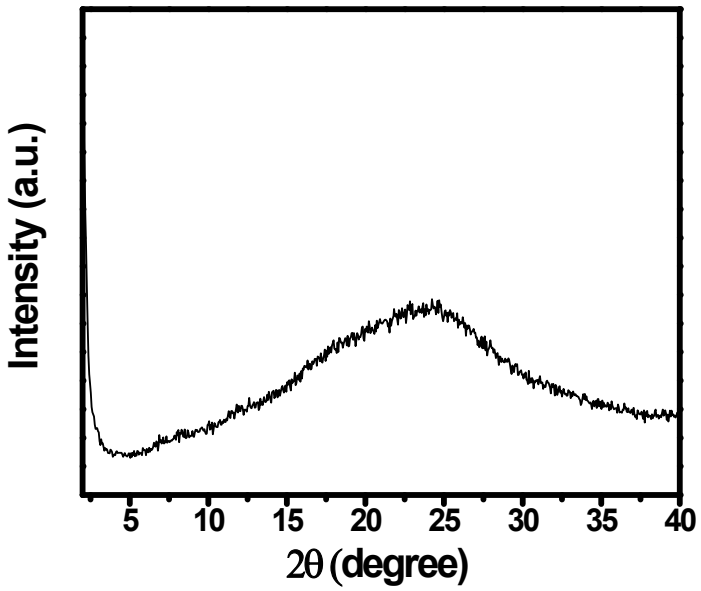

Figure S3. PXRD plot of **PER@NiP-CMOP-1**

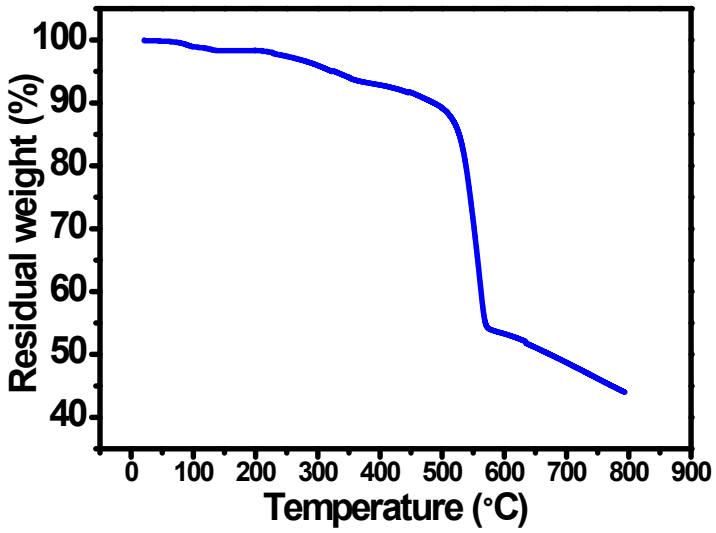

Figure S4. TGA-DTA plot of **PER@NiP-CMOP-1**

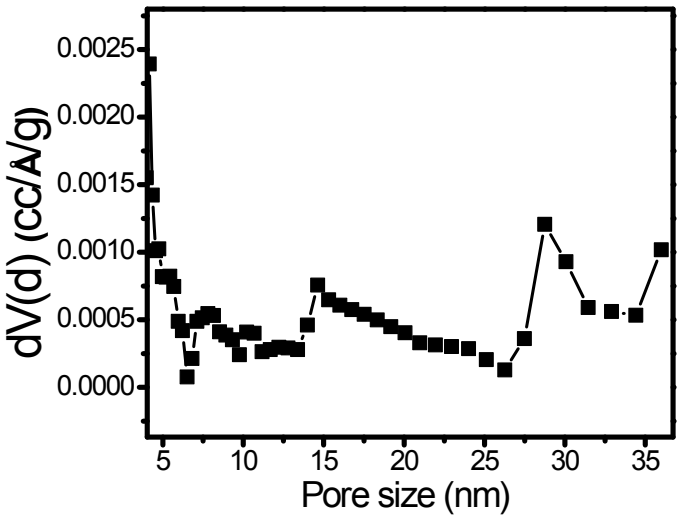

Figure S5. ^{13}C solid state CP-MAS NMR of **PER@NiP-CMOP-1**

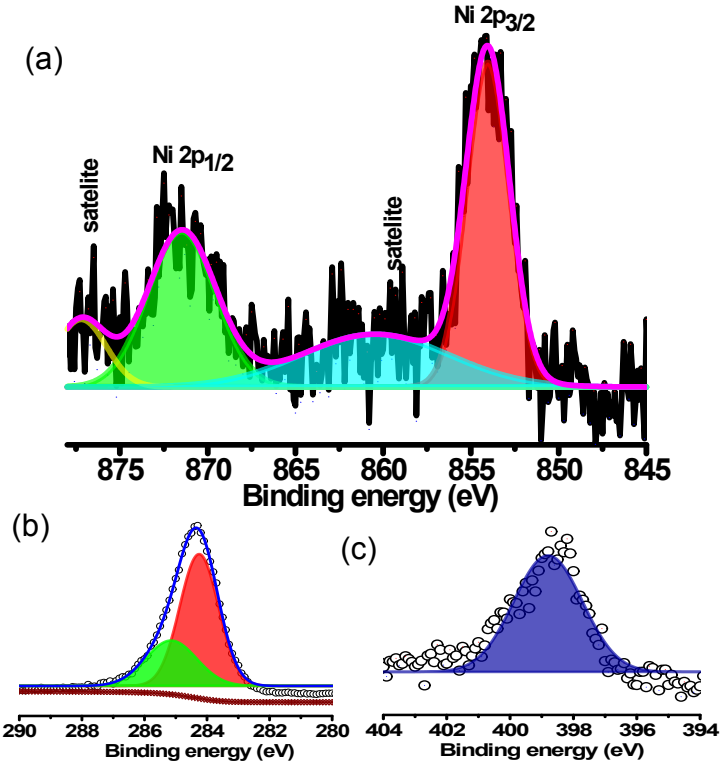

Figure S6. XPS of Ni^{2+} (a), C1s (b) and N1s (c) of **PER@NiP-CMOP-1**

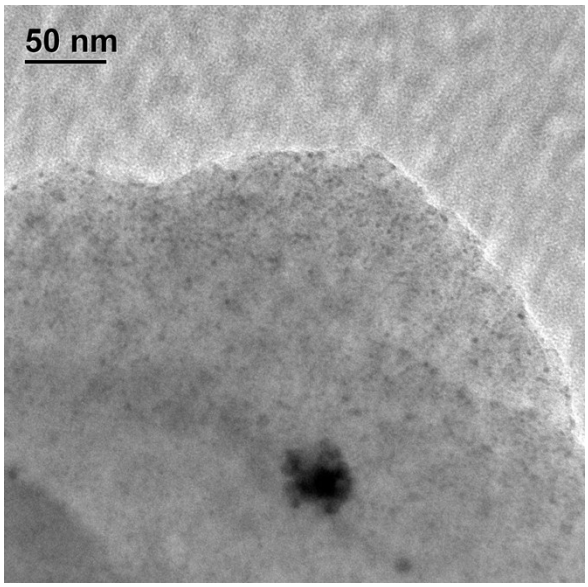

Figure S7. UHR-TEM image of **PER@NiP-CMOP-1**

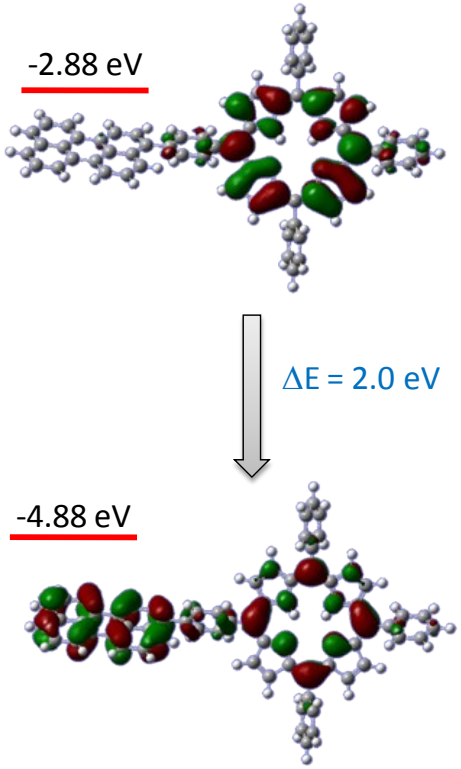

Figure S8. FMO analysis of **PER@NiP-CMOP-1** shows HOMO (below) and LUMO (top) orbitals.

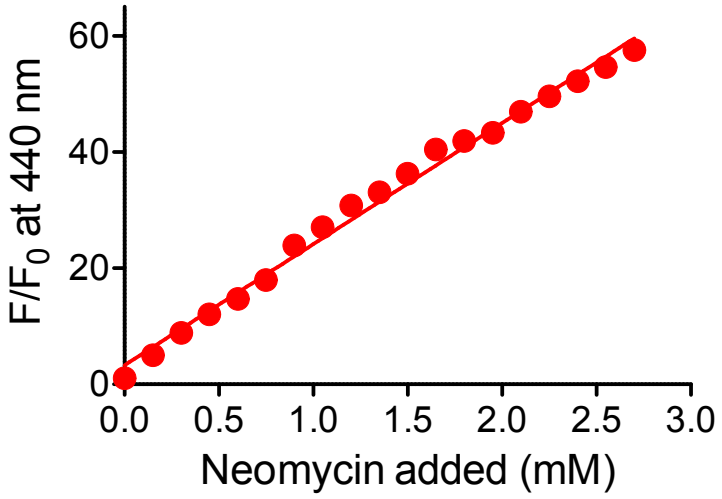

Figure S9. Change in emission intensity of **PER@NiP-CMOP-1** (20 µg/ mL, λex = 350 nm) at 440 nm upon addition of neomycin (0 – 2.7 mM) at pH 7.4 in Tris-HCl buffer [Number of independent measurement 3].

Detail procedure for calculating detection limit

A solution of **PER@NiP-CMOP-1** at pH 7.4 in water showed an increase in emission intensity at 440 nm band upon addition of neomycin (0-2.25 mM). Therefore measurements have been carried out at this wavelength for calibration. Overall 18 measures and 10 blank replicates were used for calibration.

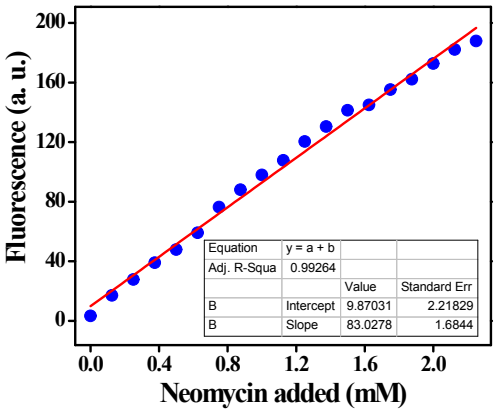

Conc. of neomycin (mM)	F. I. at 440 nm	Conc. of neomycin (mM)	F. I. at 440 nm
0	3.38	1.25	120.45
0.125	17.15	1.375	130.46
0.25	27.84	1.5	141.35
0.375	39.08	1.625	144.93
0.5	47.84	1.75	155.28
0.625	59.19	1.875	162.21
0.75	76.45	2	172.72
0.875	88.10	2.125	182.19
1	98.03	2.25	187.88
1.125	107.72		

Figure S10. Titration plot of **PER@NiP-CMOP-1** with neomycin at 440 nm wavelength

PER@NiP-CMOP-1 concentrations were calculated from the equation 1 as obtained from the calibration curve (a straight line) (fig. SX).

Y = 83.0278 x + 9.8703…….(1)

Then these calculated neomycin concentrations, represented as [neomycin]calcd. were plotted against actually added PER@NiP-CMOP-1, represented as [neomycin]actual. Slope (b) of this plot (fig. SX) was further used for calculating the detection limit in terms of concentration.

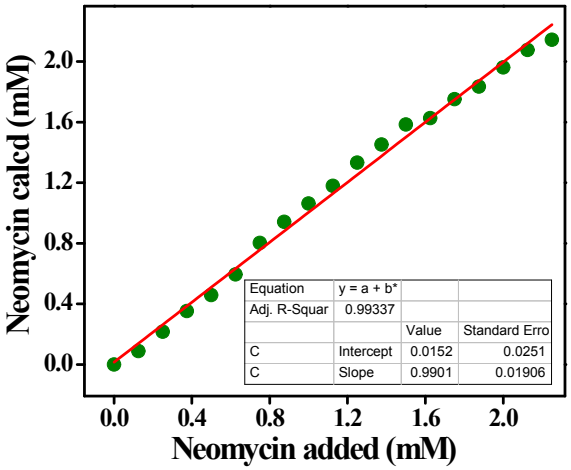

Figure S11. New calibration plot

Thereafter, from the measured blank emission values of **PER@NiP-CMOP-1** (20 µg/mL, λex = 340 nm), the concentrations of PER@NiP-CMOP-1 were calculated using the equation [1]. The mean (x) and the standard deviation (s) from the PER@NiP-CMOP-1 concentrations as calculated from the blank replicates are,

$(x \pm s) = (-0.08197 + 5.793) \times 10^{-5}$ …… [2]

The decision limit (Lc) was calculated using equation [3].

$Lc = tc \times s \times (1 + 1/N)^{1/2}$.....[3]

The probability level of 5% was calculated using equation [4], where t_c will be 1.833 for 9 degrees of freedom (GL = N-1 = 10-1 = 9) and N denotes the number of blank replicates.

So, in the present case, considering N = 10, we obtain,

$L_c = 1.833 \times (5.793 \times 10^{-5}) \times (1 + 1/10)^{1/2} = 11.15 \times 10^{-5}$ …….... [4]

The detection limit (L_D) is considered as the double of the decision limit (Equ. 5),

$LD = 2 \times Lc = 22.30 \times 10^{-5}$ ……..[5]

The detection limit (x_D) in concentration was calculated using equation [6],

$x_D = 2xc = 2\ Lc/b = (22.30 \times 10^{-5})/0.994 = 22.4 \times 10^{-5}$ mM……..[6]

Thus, the detection limit for PER@NiP-CMOP-1 is obtained as 2.24 x 10^{-7} mM.

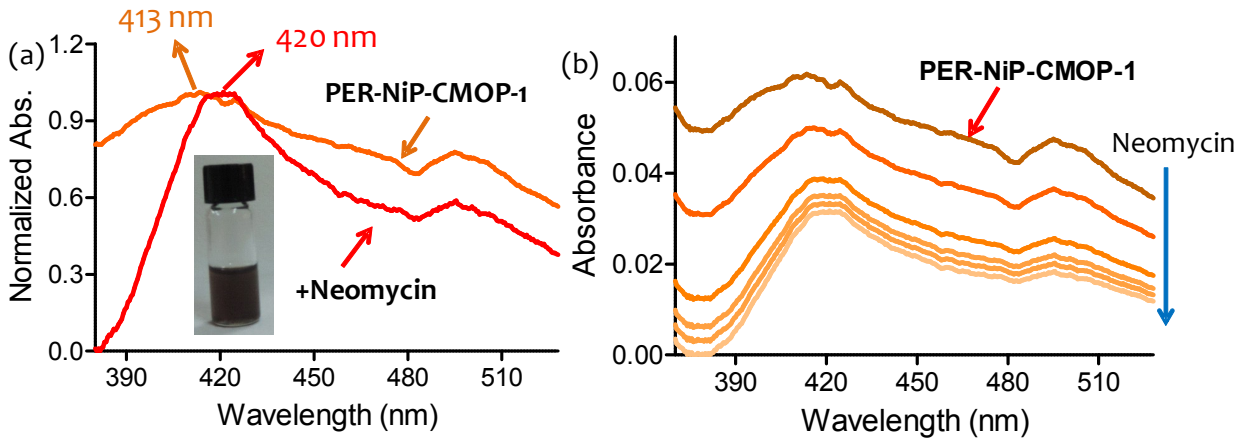

Figure S12. (a) UV-visible spectra of **PER@NiP-CMOP-1** (20 µg/ mL) in presence and absence of neomycin (2.25 mM) at pH 7.4 in Tris-HCl buffer. (Image shows well-dispersed solution of **PER@NiP-CMOP-1** at pH 7.4 in Tris-HCl buffer). (b) UV-visible titration of **PER@NiP-CMOP-1** (20 µg/ mL) with neomycin (0-2.25 mM) at pH 7.4 in Tris-HCl buffer.

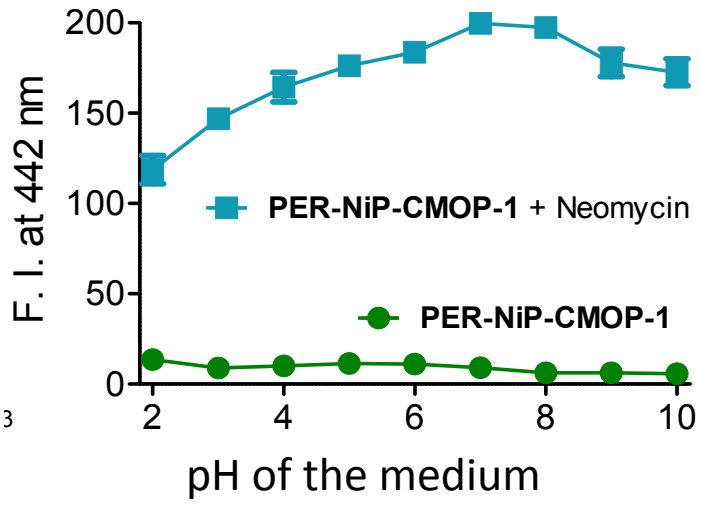

Figure S13. Effect of pH on the interactions of **PER@NiP-CMOP-1** (20 µg/ mL, λex = 350 nm) with neomycin (2.25 mM) [Number of independent measurement 3] in different buffered medium.

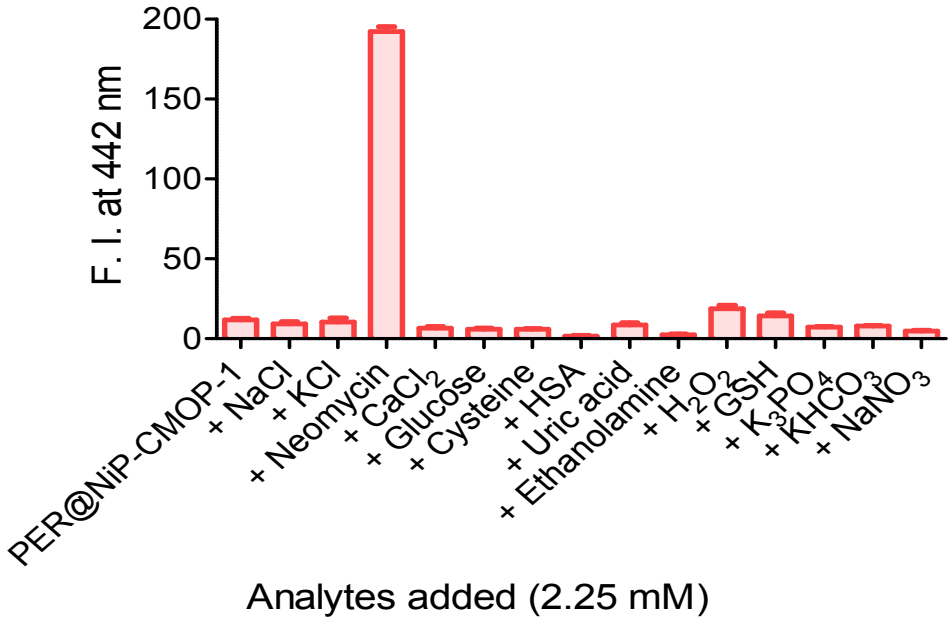

Figure S14. Change in emission intensity of **PER@NiP-CMOP-1** (20 µg/ mL, λex = 350 nm) at 442 nm in presence of different biologically relevant analytes (2.25 mM) at pH 7.4 in Tris-HCl buffer [Number of independent measurement 3].

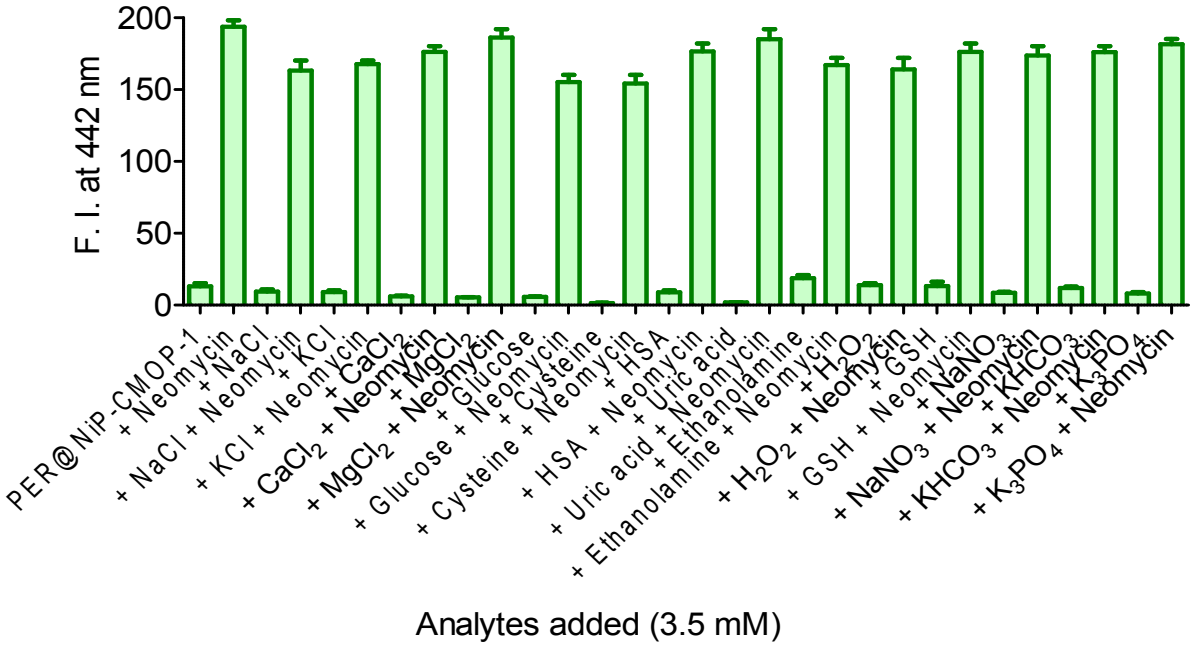

Figure S15. Change in emission intensity of **PER@NiP-CMOP-1** (20 µg/ mL, λex = 350 nm) at 442 nm upon addition of neomycin (2.25 mM) in presence of excess of other analytes (3.5 mM) at pH 7.4 in Tris-HCl buffer [Number of independent measurement 3].

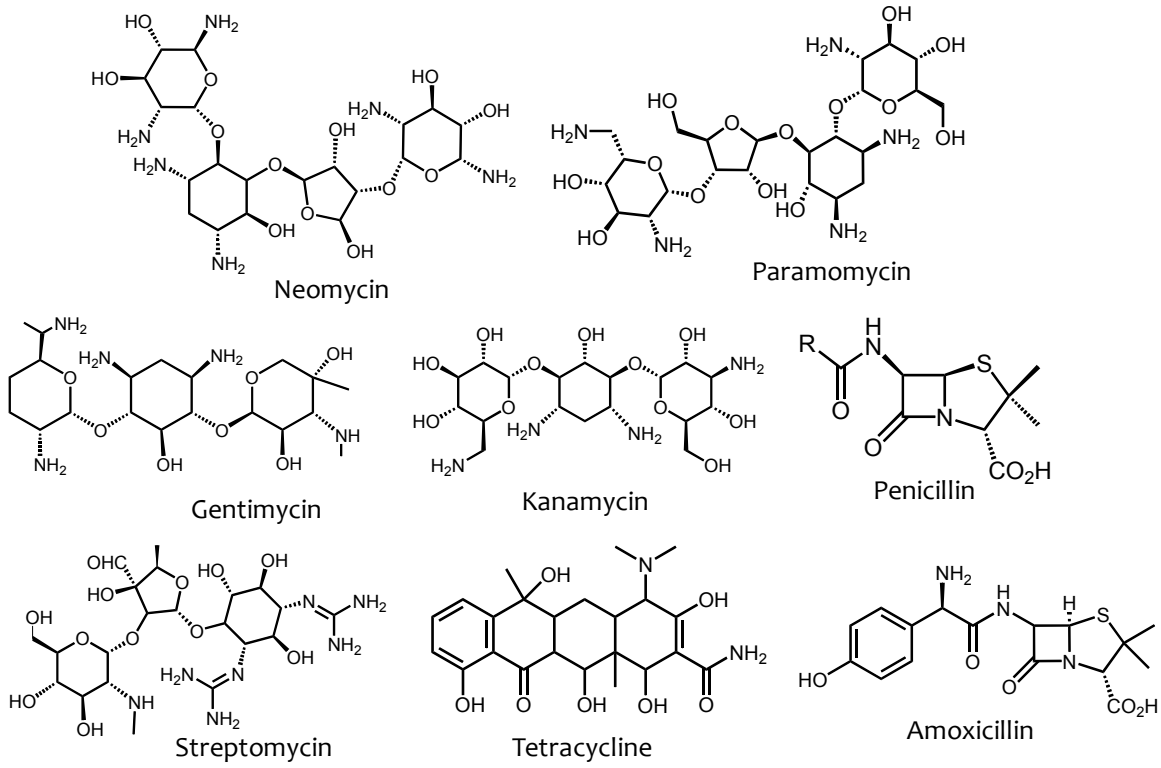

Figure S16. Structures of aminoglycoside and non-aminoglycoside antibiotics involved in present study.

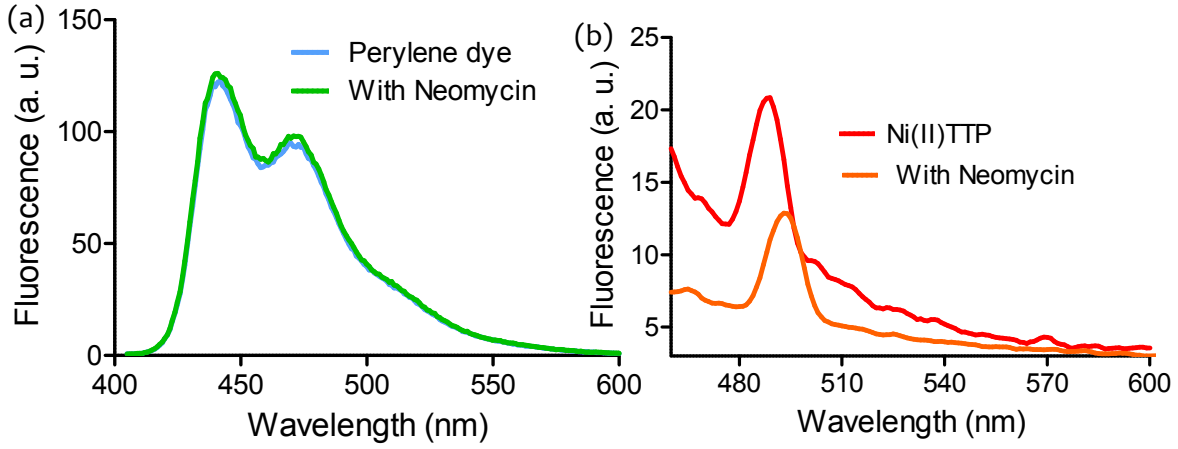

Figure S17. (a) Emission spectra of perylene dye (20 µg/ mL, λex = 405 nm) in presence of neomycin (2.25 mM) at pH 7.4 in Tris-HCl buffer. (b) Emission spectra of Ni(II)-porphyrin dye (20 µg/ mL, λex = 420 nm) in presence of neomycin (2.25 mM) at pH 7.4 in Tris-HCl buffer.

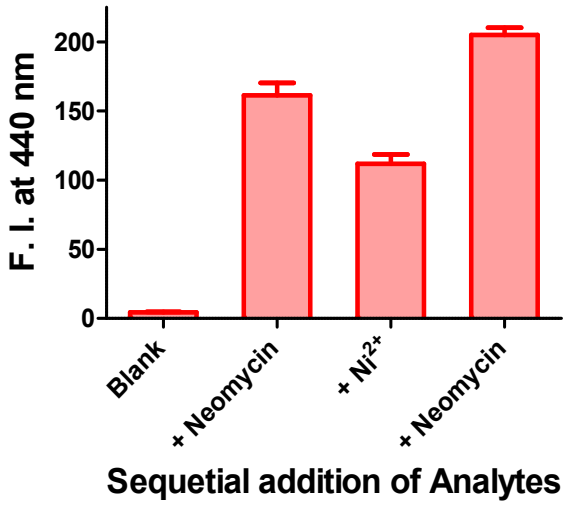

Figure S18. Change in emission intensity of **PER@NiP-CMOP-1** (20 µg/ mL, λex = 350 nm) at 442 nm upon sequential addition of neomycin (2.25 mM) and Ni^{2+} (6.75 mM) in the same solution at pH 7.4 in Tris-HCl buffer [Number of independent measurement 3].

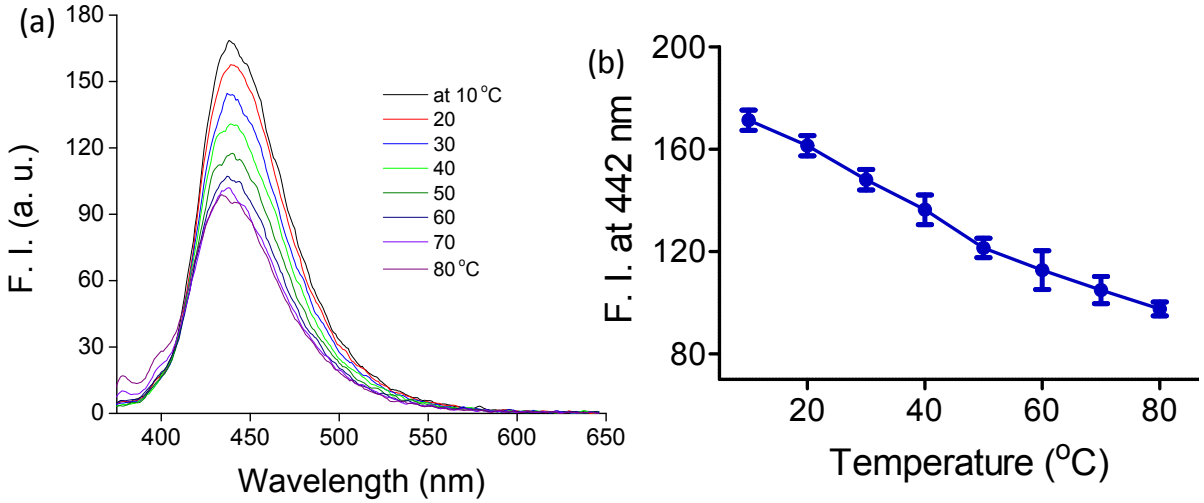

Figure S19. (a) Temperature-induced change in emission spectra of **PER@NiP-CMOP-1** (20 µg/ mL, λ_{ex} = 350 nm) at pH 7.4 in Tris-HCl buffer. (b) Change in emission intensity of **PER@NiP-CMOP-1** (20 µg/ mL, λex = 350 nm) upon variation of temperature (10 – 80°C) at pH 7.4 in Tris-HCl buffer [Number of independent measurement 3].

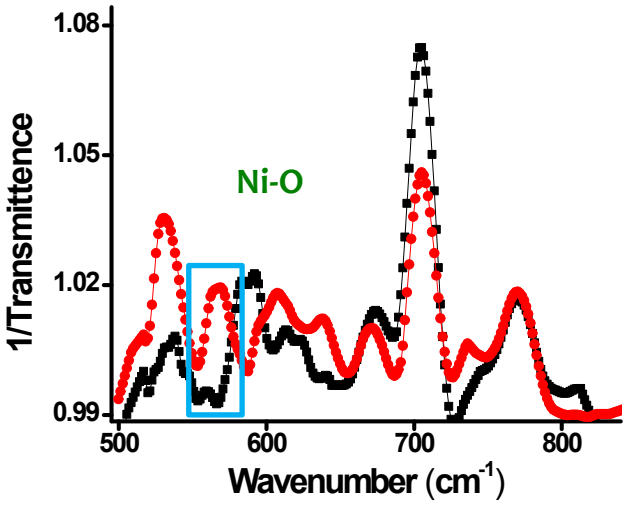

Figure S20. FT-IR spectra of PER@NiP-CMOP-1 with neomycin (2.25 mM) at pH 7.4 in water.

	T_1	A_1 (%)	T_2	A_2 (%)	T_3	A_3 (%)	<T>	X^2
1	0.56	56.8	0.27	40.1	2.52	3.10	**0.80**	1.08
1 + Neomycin	0.87	88.2			2.02	11.8	**1.14**	1.10
	Hydrogen bonding adduct		Charge transfer adduct		Monomer			

The time-dependent emission spectra of the polymer showed a tri-exponential decay profile, suggesting more complex photophysics. The relatively long-lived decay component (~2-2.5 ns) might be originated from the monomeric perylene units. The short life time component (0.27 ns) suggests the formation of charge transfer species with relatively low fluorescence quantum yield. The other time constant (0.56 ns) originates from the solvated CMP materials, where solvent

molecules induce emission quenching through high frequency vibrations of O-H functional groups. In presence of neomycin, no time constant was observed in the range ~0.2-0.3 ns, indicating the diminution of charge transfer interaction in presence of neomycin.

Table S2. Time-constants of fluorescence decay plot of **PER@NiP-CMOP-1** (20 µg/ mL, λex = 350 nm) alone and in presence of neomycin (2.25 mM) at pH 7.4 in Tris-HCl buffer.

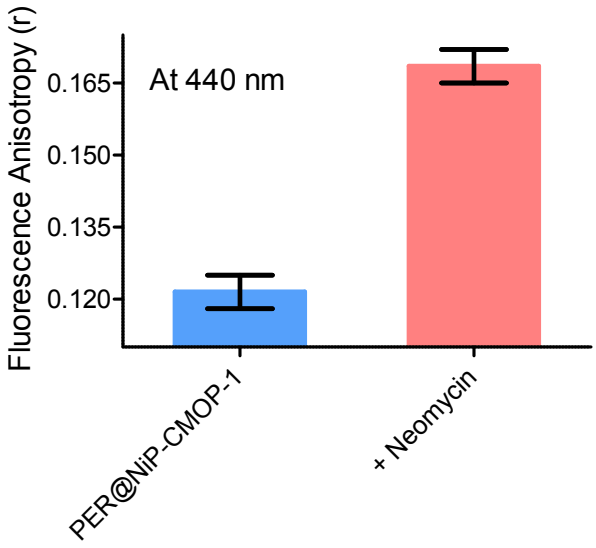

Figure S21. Fluorescence anisotropy of PER@NiP-CMOP-1 both in presence and absence of neomycin (2.25 mM) at pH 7.4 in water.

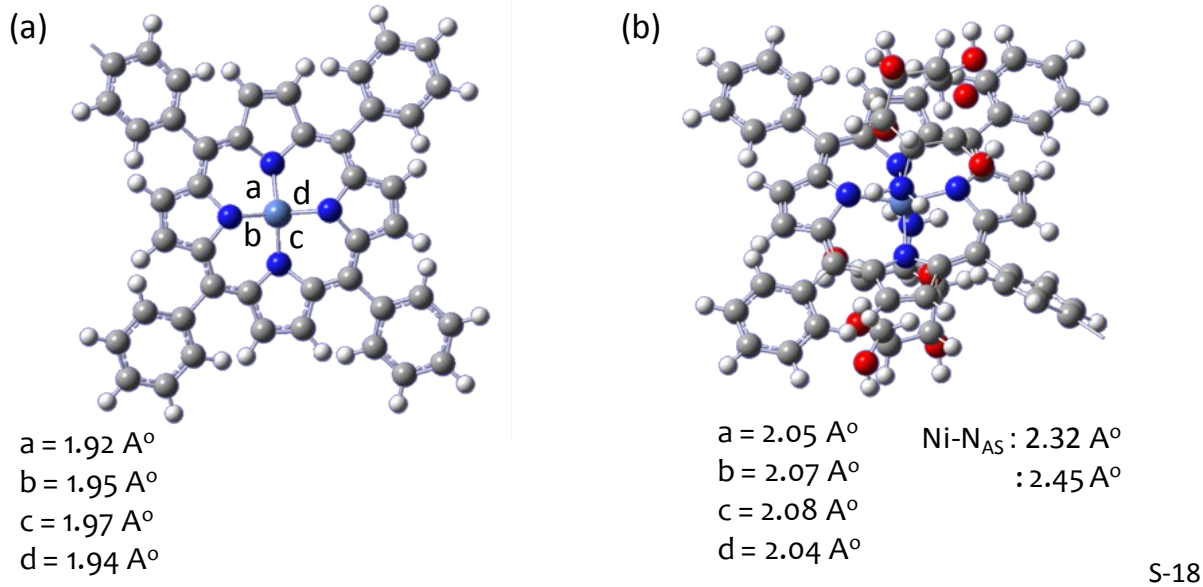

Figure S22. (a) Bond distance estimations for probe alone (a) representative fragment of **PER@NiP-CMOP-1**) by using B3LYP/6-31G* level of theory for C, H, O and N atoms and B3LYP/LANL2DZ for Ni atom. (b) Bond distance calculations for probe + glucososamine (representative for neomycin) conjugate by using B3LYP/6-31G* level of theory for C, H, O and N atoms and B3LYP/LANL2DZ for Ni atom.

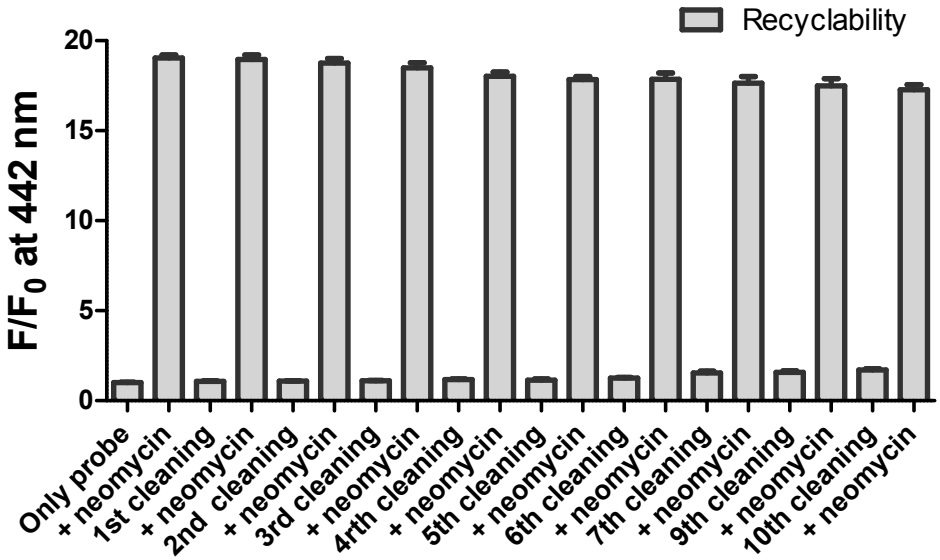

Figure S23. Recyclability of **PER@NiP-CMOP-1** (20 µg/ mL, λex = 350 nm) in sensing of neomycin (2.25 mM), change in emission was monitored at 442 nm at pH 7.4 in Tris-HCl buffer [Number of independent measurement 3]

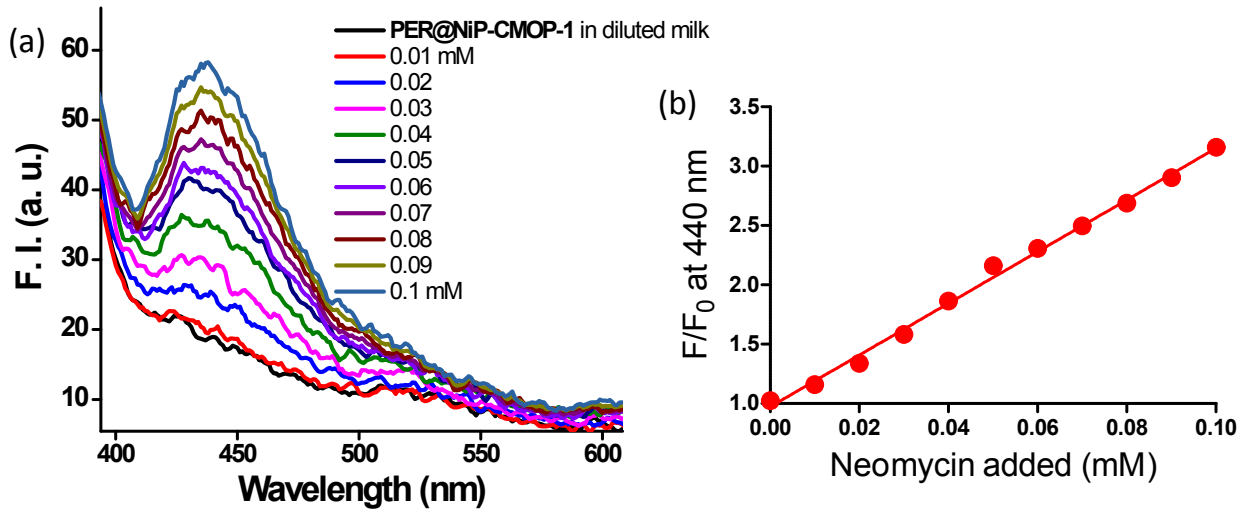

Figure S24. (a) Fluorescence titration of **PER@NiP-CMOP-1** (20 µg/ mL, λex = 350 nm) with neomycin in diluted milk solution (20% in pH 7.4 Tris-HCl buffer). (b) Change in emission intensity of **PER@NiP-CMOP-1** (20 µg/ mL, λex = 350 nm) upon addition of neomycin in diluted milk solution (20% in pH 7.4 Tris-HCl buffer) [Number of independent measurement 2]

(a)

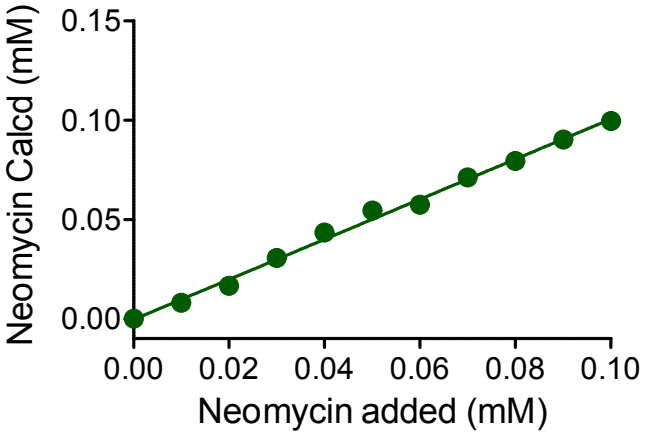

(b)

Neomycin added (mM)	Neomycin calcd. (mM) (Exp-1)	Neomycin calcd. (mM) (Exp-2)	Neomycin calcd. (mM) (Average)	Error (%)
0	0	0	0	0
0.01	0.0089	0.009	0.0090	-9.45
0.02	0.0191	0.020	0.0199	-0.025
0.03	0.0261	0.035	0.0305	1.88
0.04	0.0419	0.045	0.0434	8.64
0.05	0.0529	0.056	0.0544	8.98
0.06	0.0599	0.055	0.0574	-4.23
0.07	0.0683	0.074	0.0711	1.66
0.08	0.0767	0.082	0.0793	-0.8
0.09	0.0874	0.093	0.0902	0.23
0.1	0.0981	0.101	0.0995	-0.44

Figure S25. (a) Recovery plot shows quantitative estimation of neomycin by **PER@NiP-CMOP-1** (20 μg/ mL, λex = 350 nm) in diluted milk solution (20% in pH 7.4 Tris-HCl buffer). (b) Percentage error calculations during neomycin estimation in diluted milk solution (20% in pH 7.4 Tris-HCl buffer) [Number of independent measurement 2].

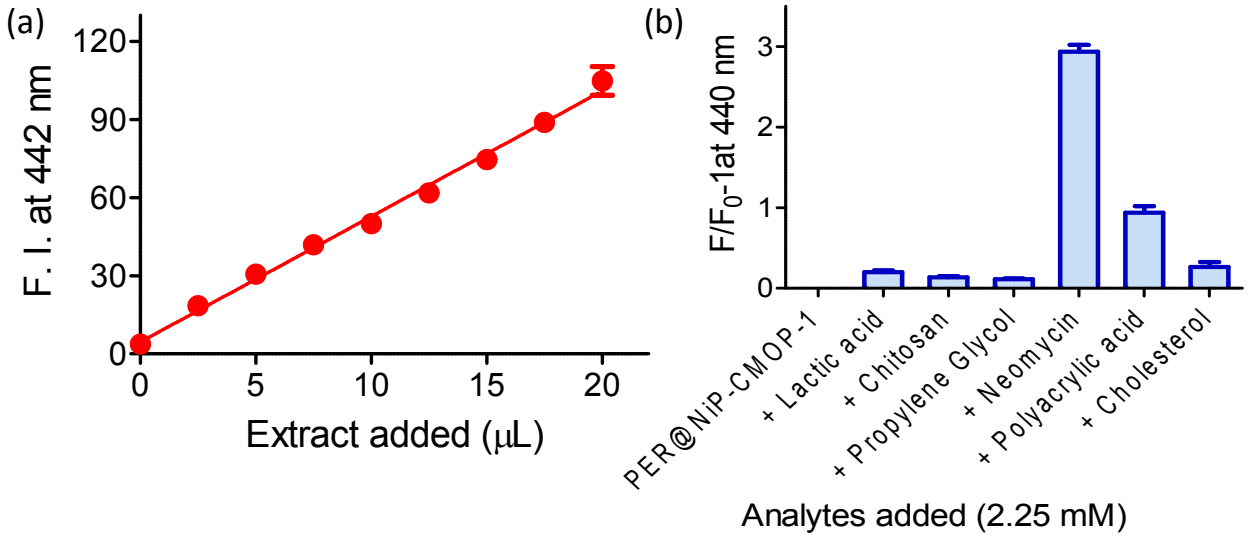

Figure S26. (a) Change in emission intensity of **PER@NiP-CMOP-1** (20 μg/ mL, λex = 350 nm) at 440 nm band upon addition of different volumes of tablet extract at pH 7.4 in Tris-HCl buffer. (b) Change in emission intensity of **PER@NiP-CMOP-1** (20 μg/ mL, λex = 350 nm) at 442 nm band in presence of other adjuvants commonly present in pharmaceutical tablet of neomycin [Number of independent measurement 2].

(a)

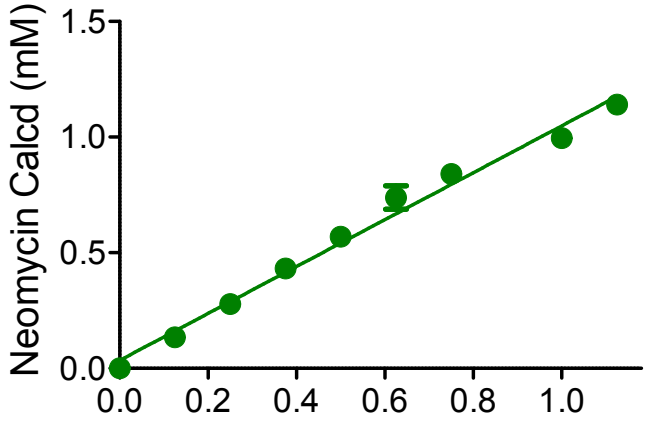

(b)

Vol of extract (µL)	Estimated conc. (mM) Exp-1	Estimated conc. (mM) Exp-2	Average value (mM)	Calcd. conc. (mM)	Percentage error (%)
0	0	0	0	0	0
2.5	0.14	0.13	0.13	0.125	4.0
5	0.28	0.27	0.28	0.25	12.0
7.5	0.43	0.41	0.42	0.375	10.5
10	0.57	0.55	0.56	0.5	12
12.5	0.65	0.69	0.67	0.625	7.2
15	0.80	0.83	0.82	0.75	9.3
17.5	0.92	0.96	0.94	0.875	7.4
20	1.18	1.15	1.17	1.12	4.7

Figure S27. (a) Recovery plot shows quantitative estimation of neomycin by **PER@NiP-CMOP-1** (20 µg/ mL, λex = 350 nm) in pharmaceutical tablet. (b) Percentage error calculations during neomycin estimation in pharmaceutical tablet [Number of independent measurement 2].

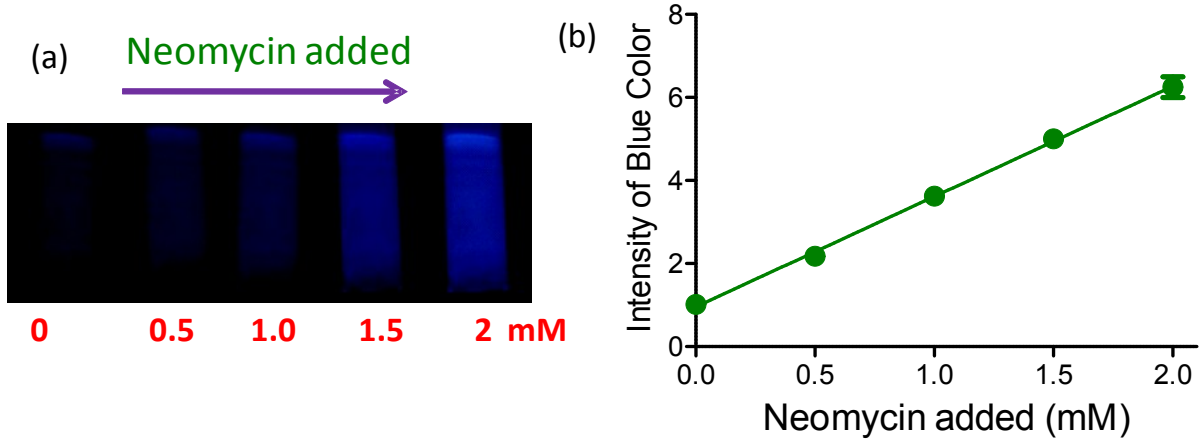

Figure S28. (a) Images of **PER@NiP-CMOP-1** immobilized paper strips under UV-lamp on treatment with different amounts of neomycin at pH 7.4 in Tris-HCl buffer. (b) Change in blue color intensity of **PER@NiP-CMOP-1** immobilized paper strips upon dipping into solutions containing different amounts of neomycin (as calculated by ImageJ software) [Number of independent measurement 2].

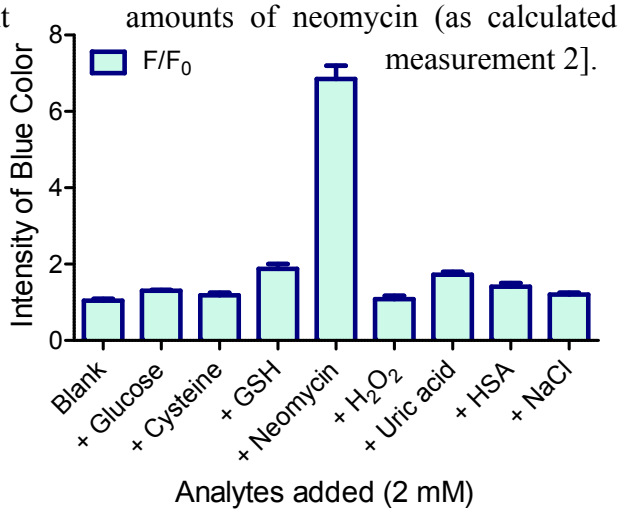

Figure S29. Images of **PER@NiP-CMOP-1** immobilized paper strips under UV-lamp on treatment with different analytes (2 mM) at pH 7.4 in Tris-HCl buffer (as calculated by ImageJ software) [Number of independent measurement 2].